

# We are IntechOpen, the world's leading publisher of Open Access books Built by scientists, for scientists

4,800

Open access books available

122,000

International authors and editors

135M

Downloads

Our authors are among the

154

Countries delivered to

TOP 1%

most cited scientists

12.2%

Contributors from top 500 universities



WEB OF SCIENCE™

Selection of our books indexed in the Book Citation Index  
in Web of Science™ Core Collection (BKCI)

Interested in publishing with us?  
Contact [book.department@intechopen.com](mailto:book.department@intechopen.com)

Numbers displayed above are based on latest data collected.  
For more information visit [www.intechopen.com](http://www.intechopen.com)



---

# High-Resolution Electric-Field-Driven Jet 3D Printing and Applications

---

Guangming Zhang, Lei Qian, Jiawei Zhao,  
Hefei Zhou and Hongbo Lan

Additional information is available at the end of the chapter

<http://dx.doi.org/10.5772/intechopen.78143>

---

## Abstract

Multi-scale and multi-material 3D printing technique has been regarded as a revolutionary technology and a next-generation manufacturing tool, which can really fulfill the “creating material” and “creating life,” especially subvert the traditional product design and the manufacturing method. However, very few of the established additive manufacturing processes possess the capability to fully implement the fabrication of multi-scale and multi-material. A novel high-resolution 3D printing, named as high-resolution electric-field-driven jet 3D printing, which is based on the induced electric field and EHD cone-jetting behavior, has been developed by our research team. It provides a feasible approach to implement the additive manufacturing of multi-scale and multi-material with high efficiency and low cost. This chapter will introduce this new high resolution 3D printing technique. In particular, many typical applications including transparent conducting electrodes, tissue engineering scaffold, 3D electronics, etc., are presented in detail.

**Keywords:** electric-field-driven (EFD) jet deposition, multi-scale 3D printing, micro-scale 3D printing, micro/nanoadditive manufacturing

---

## 1. Introduction

The manufacturing technology for multi-material and multi-scale structure has been regarded as one of the most urgent needs for the manufacturing science. The development of new functional materials (functional gradient materials, biomimetic materials, and intelligent materials), tissue engineering (tissue scaffold, and organ), and next generation electronic products

(embedded electronic products, flexible electronics, and wearable devices) has been proposing wide scientific and practical engineering requirements for the multi-material and multi-scale manufacturing technique. However, the existing manufacturing technologies are facing enormous challenges in the field of multi-material and multi-scale structure manufacturing [1–3].

3D printing has shown great potential and broad engineering application prospect in the field of multi-material and multi-scale 3D structure manufacturing due to its advantages including (1) the shape complexity; (2) the material complexity; (3) the function complexity and so on. In recent years, in order to achieve the goal of functional driven integrated manufacturing of “material-structure-devices,” 3D printing technology has been developed from traditional controlling shape to controlling properties, from printing single homogeneous material to printing multi-material or functional gradient material, from macro-scale to micro-scale or multi-scale including macro/micro/nanoscale. The functional structure electronics, as one kind of typical multi-material and multi-scale 3D printing product, which is composed of structural materials (plastics, polymers, ceramics, metals, etc.), conductive materials (the conductive silver paste, the nanosilver conductive ink, etc.), dielectric materials (various insulating materials), and semiconductor materials. The feature size of printed structure includes multi-scale (macro/micro/nanoscale) [4–10]. However, most of the existing 3D printing technologies are limited to print single material, and it is difficult to achieve the multi-scale (macro/micro/nanoscale) heterogeneous 3D structure manufacturing.

Compared with other 3D printing processes, the 3D printing technologies (inkjet printing and electrohydrodynamic jet printing) based on materials’ jet deposition have shown outstanding advantages for multi-material and multi-scale structure manufacturing. However, the inkjet printing is limited by the viscosity of printing material, which is usually less than 30cp. And the resolution of the current printed patterns is generally not more than 20  $\mu\text{m}$  of line width. The electrohydrodynamic (EHD) jet printing [11, 12], which has been proposed and developed by Park and Rogers, has much higher resolution because of the Taylor cone induced by electric field. However, there are still many shortcomings and limitations as follows: (1) The height limitation of the printed structure, it is also difficult to achieve macro/micro scale integrated printing due to the limitation of 3 mm for the distance between nozzle and substrate; (2) The insulating substrate and its thickness limitation [13]. (3) The big challenging for the conformal printing on the surface of an existing object, especially on the inclined and curved surfaces [14].

In order to solve the problems of complex 3D structure manufacturing with multi-material and multi-scale, and to achieve the integrated manufacturing with heterogeneous multi-material in macro/micro multi-scale. A novel high-resolution 3D printing, named as high-resolution electric-field-driven jet 3D printing, which is based on the induced electric field and EHD cone-jetting behavior, has been developed to provide a feasible approach to implement additive manufacturing with multi-scale and multi-material at low cost. This chapter will introduce the principle, the simulation, the experiments, and the applications of EFD jet deposition 3D printing technology.

## 2. The principle of EFD jet deposition 3D printing

### 2.1. The basic principle

The electric-field-driven (EFD) jet 3D printing system is mainly composed of a printhead, a three-axis translation stage, a high-voltage power supply, a signal generator, and a material feeding unit. **Figure 1** shows the setup schematic of the EFD jet deposition 3D printing system. The nozzle of the printhead is directly connected to the anode of the high-voltage pulse power supply for inducing an electric field. The three-axis translation stage can be programmed to provide the planar movement of the target substrate for printing patterns and up-and-down movement of the nozzle for changing the intensity of the induced electric field. Liquid materials are delivered to the printhead by the material feeding unit, which consists of a pneumatic control system and a material reservoir. The pneumatic control system can adjust the flow rate to optimize the shape of the pendent meniscus at the nozzle by changing the gas pressure. A signal generator is used to produce the modulated voltage command signal with desired frequency and duration to trigger the output of high-voltage power supply. The printing process can be recorded by a CCD camera.

Differing from the traditional pressure-driven 3D printing and the existing EHD jet printing, the proposed technique is a liquid ejection and deposition printing based on the electrostatic induction and EHD cone-jetting. The fundamental principle of the EFD jet 3D printing is illustrated in **Figure 2**. The printing process can be described as follows:

1. With the movement of the nozzle with a high electric potential to the target substrate, the interaction between the nozzle and the substrate will be stronger and stronger by the effect of electrostatic induction. Then, an induced electric field will be generated between the nozzle and the substrate, as shown in **Figure 2(a)**.
2. The pendent meniscus induced by the gas pressure at the nozzle will be affected by the electric field causing the accumulation of the positive charges on its surface. Under the

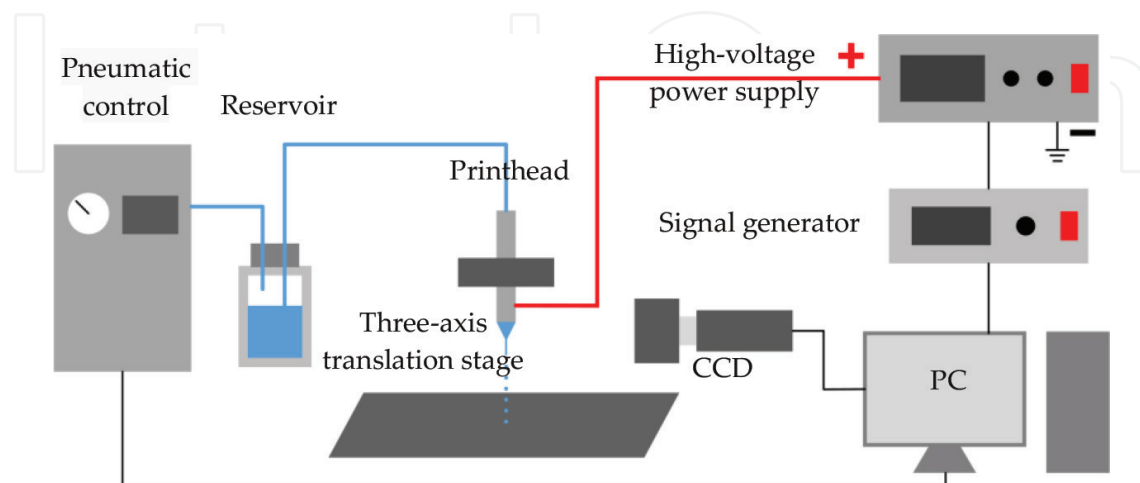


**Figure 1.** Schematic of system setup for the EFD jet deposition 3D printing.

coupling effect of the electric field force, surface tension, viscous force, and gas pressure, the meniscus will be elongated gradually to form a Taylor-cone.

3. When the tangential electric stress exceeds the surface tension during a single pulse, a droplet or fine jet from the apex of the cone will be produced. The droplet diameter and jet size are significantly smaller than nozzle size, indicating the EFD jet printing can overcome the resolution limitation from the nozzle size.
4. The simultaneous control of the ejection and movement of the printhead or substrate allows precise deposition of materials on the substrate, forming the first layer of printing object.
5. Regarding the first layer as the target substrate, then moving up the nozzle to keep the constant distance between the first layer and nozzle, a stable electric field will be reformed between the nozzle and the printed object, ensuring the stability and reliability of the process mentioned above. The thickness of the printing layer must be appropriately controlled to maintain a constant distance between the nozzle and the printed object. This process will be repeated until forming a desired 3D object.

## 2.2. The two working modes

Unlike the traditional macro-scale 3D printing and micro-scale 3D printing, the macro/micro-scale 3D printing should take into account both the printing accuracy and the printing efficiency in the printing process [15, 16]. To ensure the capability of integrated printing of multi-scale complex 3D structure, and to better meet the requirements of the practical engineering of 3D printing. We proposed two kinds of working modes for this new technique, including the pulsed cone-jet mode and continuous cone-jet mode, to achieve both high precision and high efficiency during the printing process, as shown in **Figure 3**.

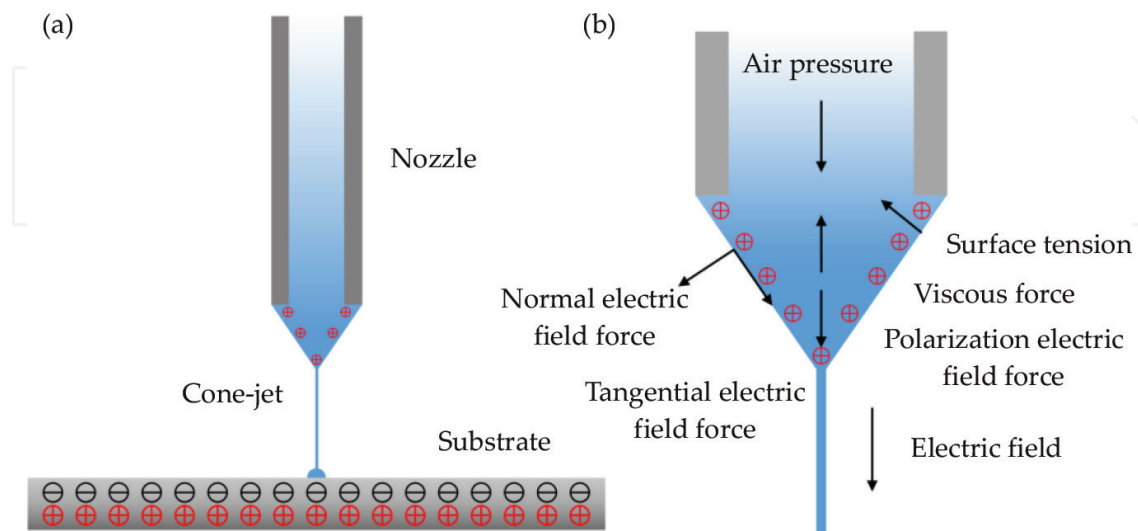


**Figure 2.** Schematic principle of the EFD jet deposition 3D printing: (a) the electrostatic induction between the nozzle and substrate; (b) stresses acting on the meniscus.

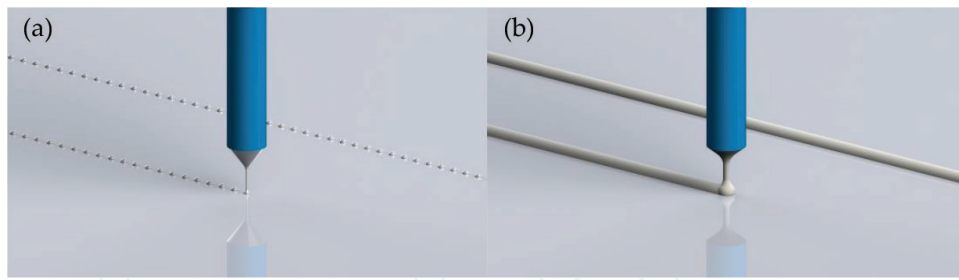


**Figure 3.** Two working modes (a) pulsed cone-jet mode; (b) continuous cone-jet mode.

1. In the pulsed cone-jet mode, the printing is a drop-on-demand process based on a pulsed voltage. When a pulsed voltage is applied, the meniscus will be deformed into Taylor-cone, and a micro-size jet is extracted to produce a micro-droplet. Then, the meniscus will be returned to the original position to produce a consistent and repeatable jet at the next pulse voltage. The printing material is deposited onto the substrate or the printed objects in the form of dots. The size of the printed dots is determined by process parameters involving the applied voltage, pulse duration time, and gas pressure, etc. The dots' spacing is mainly determined by the pulse interval time and the moving speed of the X-Y stage.
2. In the continuous cone-jet mode, the DC-voltage is applied to drive and maintain the ejection behavior. The continuous liquid with a constant flow rate is rapidly pulled from the nozzle by the electric field force. Therefore, the printing material can be deposited on the substrate or the printed object in the form of lines (similar to FDM, but the dominant driving force is still the electric field force). Moreover, the line width is related to process parameters such as the voltage, the gas pressure, and the stage velocity, etc. The continuous cone-jet mode, based on continuous printing, possesses the ability of manufacturing large-area patterns and macro/micro-scale structures compared to the pulsed cone-jet mode.

Therefore, the proposed EFD jet deposition 3D printing possesses the following advantages: (1) suitable for both conductive and non-conductive (or insulating) substrates; (2) breaking through the height limitation of printed structures of traditional EHD jet printing; (3) it can be widely used for various printing materials with large range of viscosity; and (4) it also can be used to print on the uneven surface and the conformal surface.

### **3. The numerical simulation and experiments verification**

In order to further reveal the injection molding mechanism and influencing rules of the processing parameters for EFD jet deposition 3D printing technology, this part will be focused on the investigation of printing performance under different conditions by means of numerical simulation and experimental verification. For the numerical simulation, the properties of substrate (or the printed layers), the printing height, and the variety of printing materials have been studied by the finite element simulation software (COMSOL MULTIPHYSICS), and the simulation results are verified by experiments. The results can be seen as follows.

### 3.1. The effects of different substrate materials

In order to display the electrostatic induction between the nozzle and the substrate, the intensity and the distribution of the electric field around nozzles under four different kinds conditions (no substrate, PET substrate, glass substrate, and copper substrate) were studied by finite element simulation. The relative permittivity of PET, glass, and copper substrate is 4, 10, and 1, respectively.

The simulation results of distribution and intensity of electric field with different substrates were shown in **Figure 4**. The color represents the intensity of electric field, and the arrow indicates the direction of the electric field. As shown in **Figure 4**, under the condition of no substrate, the electric field emitted by the conductive nozzle diverges anywhere, and the intensity of the electric field at the tip of the nozzle is small. While under the conditions with substrates, it can be seen that the electric field from the conductive nozzle is terminated on the surface of the substrate, and the electric field strength between the conductive nozzle and the substrate is significantly enhanced, and the electric field intensity at the tip of the nozzle is more obvious. In these four conditions, the intensities of electric field at the tip of the nozzle are 618.1, 2794.8, 2794.9 and 3227.8 V/mm, respectively. The intensity of electric field on the copper substrate is significantly higher than that of the other three cases.

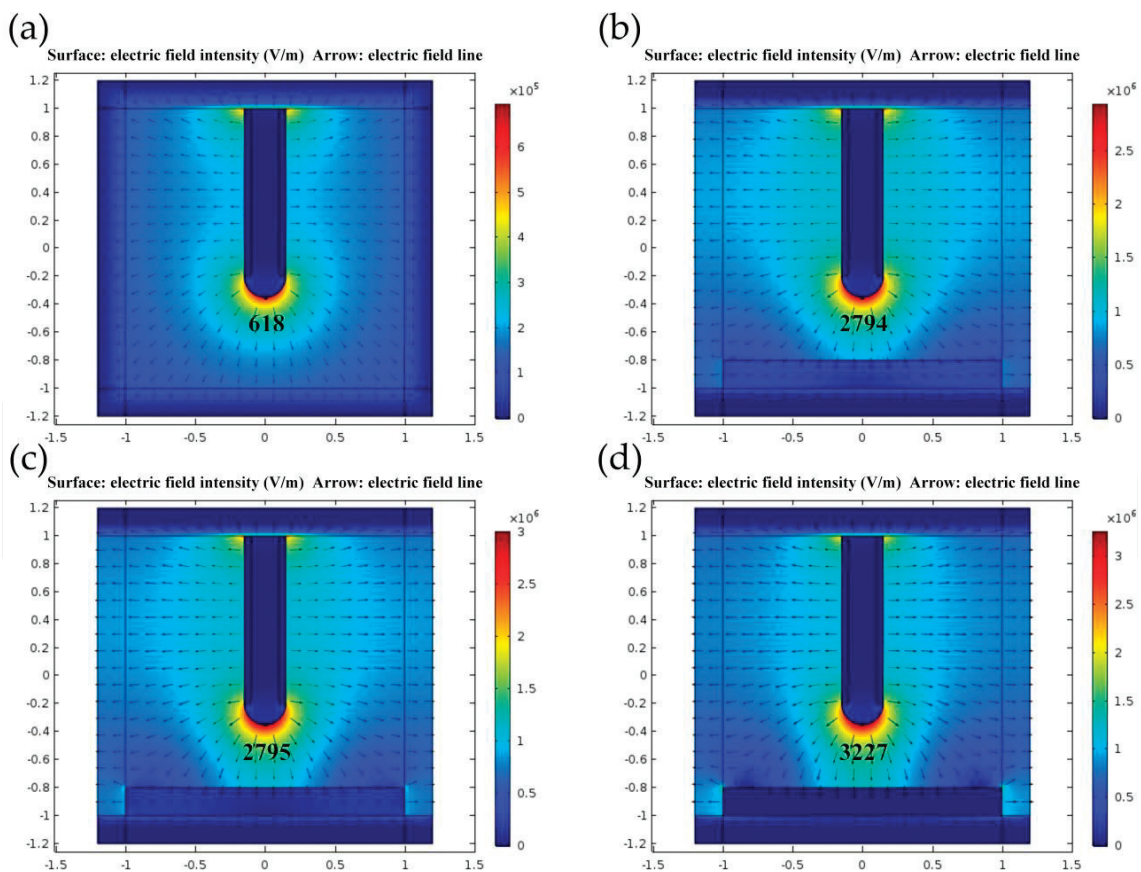


**Figure 4.** The simulation results of electric field under different substrate conditions: (a) no substrate, (b) PET, (c) glass, and (d) copper.

The reason why the substrate can change the electric field distribution is that the charges inside the substrate will redistribute by the effect of the electric field. For conductive substrate, there are lots of free charges inside the conductor, which can move freely inside the conductor. While for the insulating substrate such as PET and glass, only small amount of movable free charges can be found inside the insulating substrate, and most of charges are bounded in micro-displacement. Therefore, the electrostatic induction of the dielectric substrate is weaker than that of conductive substrate. When the conductive substrate stays in the condition of electrostatic balance, a large amount of free charges are gathered on the surface of the conductive substrate, which makes the direction of the electric field from the nozzle change to the conductive substrate. Therefore, a stronger electric field can be obtained between the nozzle and conductive substrate to provide a greater driving force for droplet jetting.

Compared with the existing EHD jet printing, the EFD jet deposition 3D printing has better applicability for different substrate materials. The EHD jet printing technology usually requires good conductivity of the target substrate, otherwise the insulating substrate with a thickness limitation must be placed on a grounding conductor. The EFD jet deposition 3D printing technology can be used in any material of substrates because the electrostatic induction can be generated in various materials, which is not limited by the conductivity or dielectric properties of the substrate. **Figure 5** shows that the Taylor cone and stable cone jet can be formed at the nozzle by using for different material substrates (conductive stainless steel, semiconductor silicon chip, and insulating glass). The distance between the tip of the nozzle and the substrate is set as 2 mm, and the printing material is low viscosity resin (100 mPa.s). The critical voltage of cone jet for conductive stainless steel, semiconductor silicon chip, and insulator glass are 2100, 2500, and 3000 V.

The experimental results show that the EFD jet deposition 3D printing is suitable for many types of substrates. And the critical voltage needed for the conductive substrate is smaller than that for the insulating substrates, which is consistent with the simulation results. Therefore, the conclusion can be proposed that the EFD jet deposition 3D printing can greatly expand the scope and the field of applications.

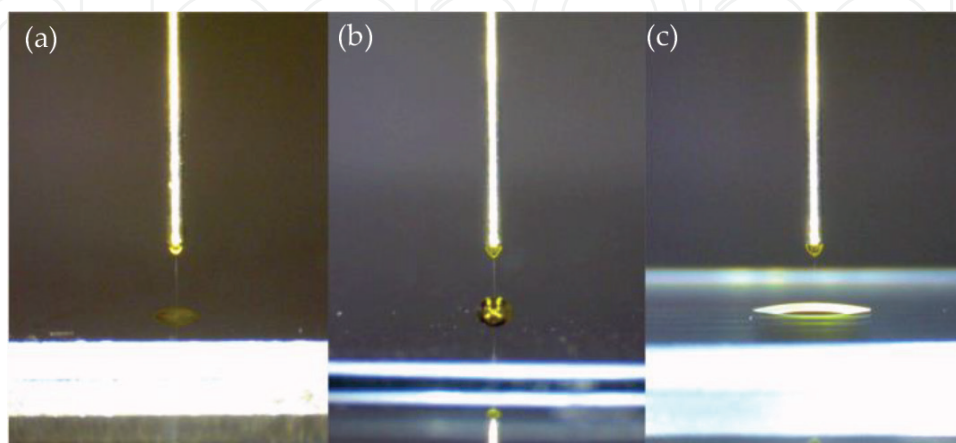


**Figure 5.** Different target substrates (a) copper plate; (b) silicon plate; and (c) glass plate.



### 3.2. The effect of different distance between nozzle and substrate

The distance between the nozzle and substrate is another key parameter for the EFD jet deposition 3D printing, which has an important impact on printing results. The effect of distance ranging from 0.4, 0.3, 0.2, and 0.1 mm on the electric field were simulated by COMSOL software, as shown in **Figure 6**. The intensity of electric field on the droplet surface is 3376.8, 3816.3, 4669.5 and 6910.5 V/mm, respectively. It can be seen that with the decrease of distance, the electric field formed between the conductive nozzle and the substrate is much enhanced, especially at the tip of the nozzle.

Due to the distance limitation between the conductive nozzle and the conductive substrate (or conductor under insulating substrate), the maximum distance of the EHD jet printing technology is usually not more than 3 mm, This caused great challenges in the macro/micro scale manufacturing for EHD jet printing. The EFD jet deposition 3D printing technology has broken through the distance limitation of the traditional EHD jet printing, and can truly realize the macro/micro-scale manufacturing. When the high voltage power is applied to the conductive nozzle, the required electric field can be formed between them under the action of electrostatic induction only if moving nozzle closed to the target substrate (or the printed layers). Therefore, this proposed technology can print on any structure surface.

The experiments have been done to investigate the stability of the Taylor cone shape and the cone jet in the printing process influenced by the substrate thickness, as shown in **Figure 7**.

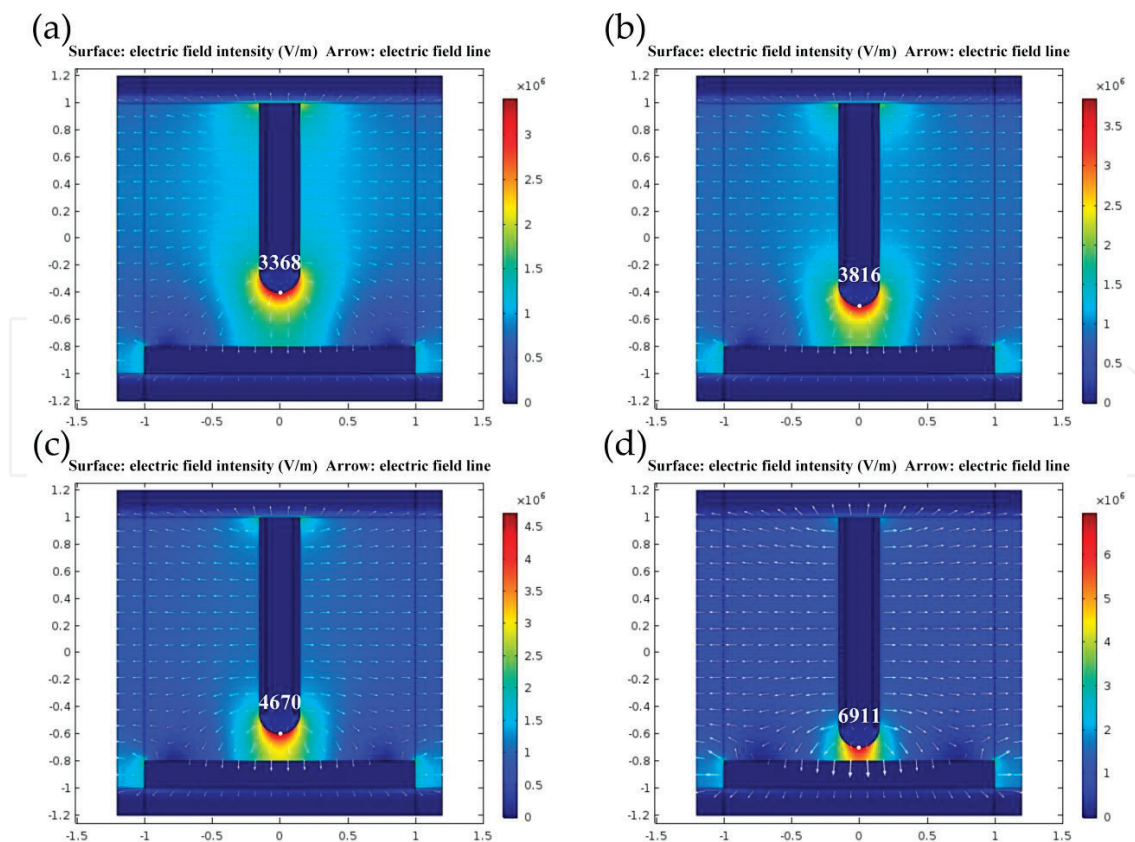


**Figure 6.** The simulation results of electric field at different nozzle heights: (a) 0.4 mm, (b) 0.3 mm, (c) 0.2 mm, and (d) 0.1 mm.

During the experiments, the distance between the conductive nozzle and the glass substrate is set as 2 mm, and the printing material is low viscosity resin (viscosity 100 mPa.s), and the voltage is 3000 V. It can be observed that the thickness of glass substrate ranging from 1.2 to 12 mm, the EFD jet deposition 3D printing can achieve stable and reliable printing. The experimental results show that the EFD jet deposition 3D printing can truly achieve the 3D printing by means of electrostatic induction between the nozzle and the target substrate (or the printed layers) (Figure 7).

### 3.3. The printing materials

The available materials for EFD jet deposition 3D printing are extensive and variable, such as organic polymer materials, bio-materials, nanoscale composites, metal, and non-conductive materials. Furthermore, the viscosity range of the printing materials is very broad because of the enough electric stress provided by the strong electric field to drive jetting. The line patterns with high resolution and high quality (line-width roughness) have been well produced

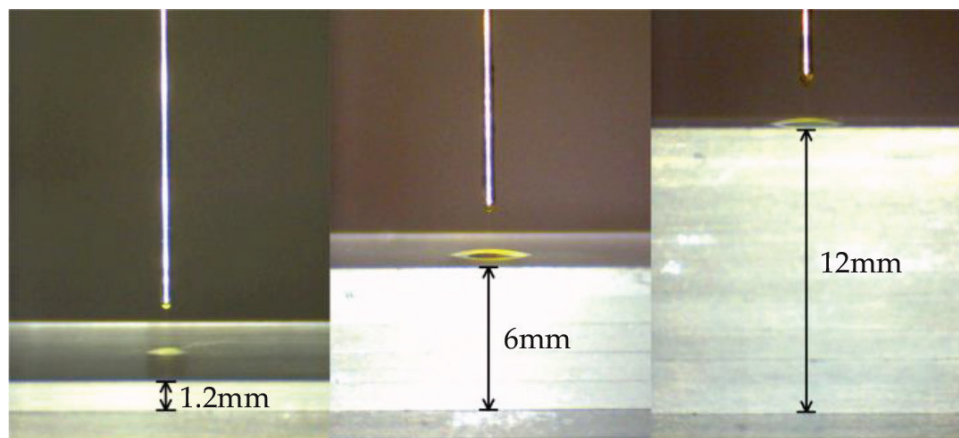


Figure 7. Reliably printing in variable heights and locations of printhead.

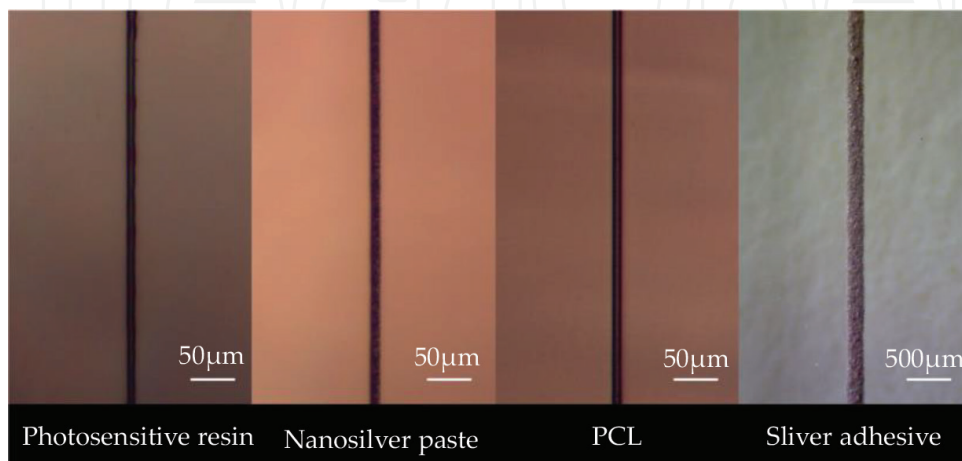


Figure 8. The features printed with various printing materials.

using four different types of materials, including the photosensitive resin, nanosilver conductive paste, polycaprolactone (PCL), and conductive silver adhesive, as shown in **Figure 8**.

The materials in the experiment have different fluidic properties and the viscosity. The viscosity of the photosensitive resin is 800 cP while the viscosity of nanosilver conductive paste is 5000 cP. The heating system was used for molding of PCL because of its solid-state at RT. The nozzle with an inner diameter of 250  $\mu\text{m}$  is adopted to print objects with a line width of 10  $\mu\text{m}$ , where the reduction ratio in dimensions between the nozzle and the printed line reaches 25:1.

The viscosity of the conductive silver adhesives at ambient temperature is 8000 cP, the inner diameter of the nozzle is 250  $\mu\text{m}$ , the line width of the object to be printed is 200  $\mu\text{m}$ , and the print patterns must have good morphology. The results showed that the EFD jet 3D printing is suitable for almost any materials, compared to existing 3D printing technology. It is unexamined for its potential to provide high-resolution (that is,  $\sim 10\mu\text{m}$ ) patterning of materials with ultra-high viscosity.

## 4. The applications of EFD jet deposition 3D printing

In this part, four typical printed structures were used to present the applications of EFD jet deposition 3D printing in multi-scale and multi material 3D printing: (1) lines and dots (one-dimensional structure); (2) high aspect ratio micro-scale “wall” structure (two-dimensional structure); (3) high resolution tissue engineering scaffold (3D structure); (4) 3D structure electronics (multi-scale and multi-material heterogeneous 3D structure).

### 4.1. Lines and dots (one-dimensional structure)

The droplet can be precisely deposited at the designated position by controlling the process of droplet jetting and the movement of stage. A dot array with the resolution of 50-60  $\mu\text{m}$  and the different dot spacing has been printed to show the capability of drop-on-demand printing in the pulsed cone-jet mode, as shown in **Figure 9(a)**. The dots' spacing decreases correspondingly with the decreasing of stage moving speed. Using the continuous cone-jet mode, a line

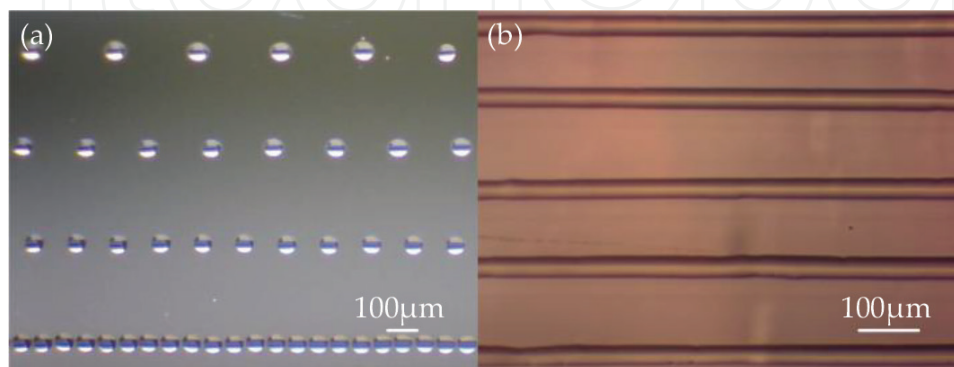


**Figure 9.** Dot and line arrays.

pattern has been successfully printed on a glass slide, as shown in **Figure 9(b)**. The average line width in this pattern is about  $40\ \mu\text{m}$ , and the line pitch is about  $150\ \mu\text{m}$ . Due to the ability of depositing materials directly as desired patterns on the substrate with a simple fabrication process and high efficiency, the proposed printing method can be adapted for applications in thin-film transistors, optical elements, organic light-emitting diodes, photonics crystals, and DNA microarrays.

By using the conductive nanosilver paste, the proposed printing method can be applied for fabrication of metal-mesh patterns used in various electronics such as flexible displays, solar cells, touch panels, etc. **Figure 10** shows the optical images of the printed metal-mesh patterns. The line width and spacing of the metal mesh in **Figure 10(a)** are  $20\ \mu\text{m}$  and  $250\ \mu\text{m}$ , respectively. And the line width and spacing in **Figure 10(b)** are  $10\ \mu\text{m}$  and  $150\ \mu\text{m}$ , respectively. The line resolution of the printed metal-mesh patterns is less than  $20\ \mu\text{m}$ , which is almost invisible to the naked eye. It indicates that the proposed technology is promising to fabricate an invisible fine transparent electrode with good electricity and optical properties, which can be widely applied to electronic devices without any cosmetic issues due to the appearance of metal pattern.

#### 4.2. The micro-scale “wall” structure (two-dimensional structure)

The EFD jet deposition 3D printing technology is mainly used for liquid printing materials, it also can be used for printing molten polymer materials by changing the nozzle structure. The material feeding unit is integrated into the printhead to shorten the distance between material feeding unit and the nozzle, because solid state printing material is difficult to be delivered to the nozzle through pipeline. The double heating module is used to heat both nozzle and feeding unit. The purpose of heating feeding unit is to keep the printed material in the melting state with certain fluidity, and that of heating nozzle is to ensure the quality and precision of the printing process.

Instead of utilizing polymer solutions as the printing material, the molten EFD jet 3D printing employs molten polymers as the printing materials. Due to the printing material is PCL with a melting point of about  $60^\circ\text{C}$ . A heating module with a heating temperature of  $80^\circ\text{C}$  is utilized to melt the solid polymer into flowing melts. Moreover, the molten polymer solidifies very quickly that benefits for the layered manufacturing of high aspect ratio structures. **Figure 11**

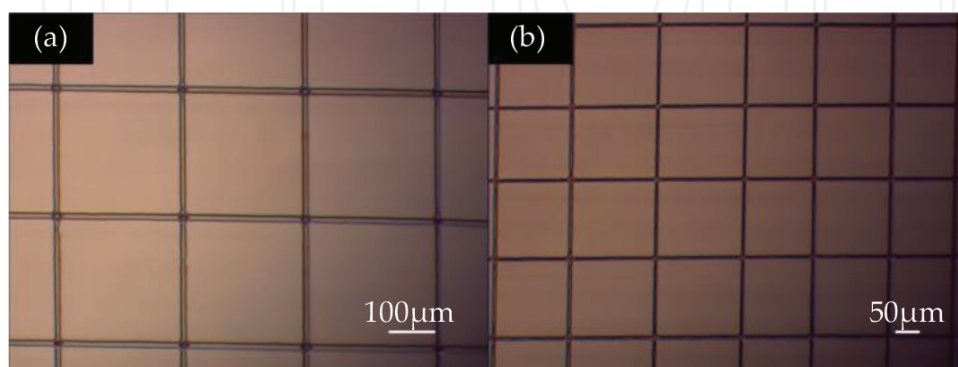


**Figure 10.** Metal-mesh patterns with (a) line width of  $20\ \mu\text{m}$  and spacing of  $250\ \mu\text{m}$ ; (b) line width of  $10\ \mu\text{m}$  and spacing of  $150\ \mu\text{m}$ .

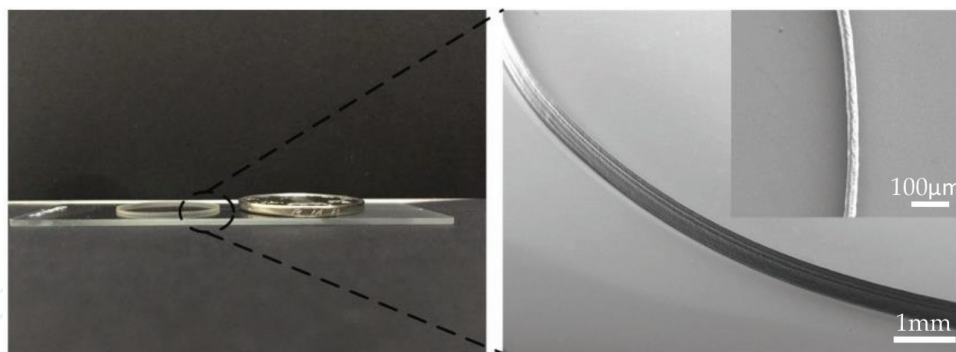


**Figure 11.** A cylinder structure with diameter of 20 mm, height of 550  $\mu\text{m}$ , and wall thickness of 20  $\mu\text{m}$ .

shows a micro-scale high aspect ratio wall structured cylinder with diameter of 20 mm, the wall thickness of 20  $\mu\text{m}$ , and the height of 550  $\mu\text{m}$  (continuous stacking of 20 layers). Compared to the traditional EHD printing, The experimental results show the molten EFD jet 3D printing offers a promising approach to produce the micro/nanostructures with ultra-high aspect ratio at low cost and high throughput.

#### 4.3. Tissue engineering scaffold (3D structure)

A typical macro/micro-scale tissue engineering scaffold is a 3D porous structure for transporting nourishment and excreting metabolites for cell growth. A desirable scaffold is characterized by controllable porosity, pore size, and pore distribution, which can provide cells with sufficient oxygen and nutrient supply. It is challenging for the current manufacturing technologies to the fully controlled orderly morphology and accuracy as requested. Polycaprolactone (PCL) with good bio-degradable performance serves as the printing material of the biological scaffold, a molten EFD jet 3D printing was employed to fabricate 3D scaffold, as shown in **Figure 12**. The printing process parameters are set as follows: voltage 2.8kV, pressure 20 kPa, moving speed 5 mm/s, and heating temperature of 80°C. The overall size of the scaffold is 4 mm x 4 mm, the line width is 60  $\mu\text{m}$ , the period is 300 m, and the height is 300  $\mu\text{m}$ , shown in **Figure 13**. The experimental results confirm that the EFD jet deposition 3D printing possesses a very prominent ability for the macro/micro scale printing.

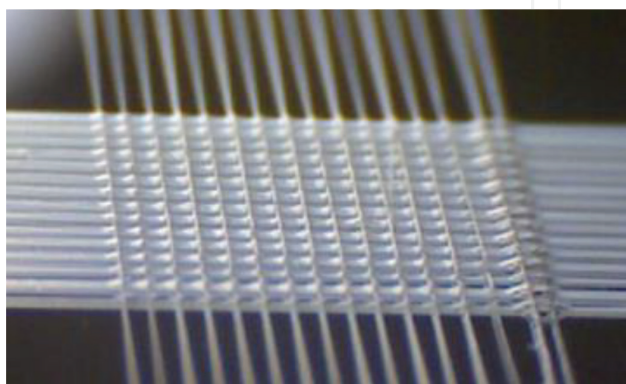


**Figure 12.** The macro view of a tissue engineering scaffold.

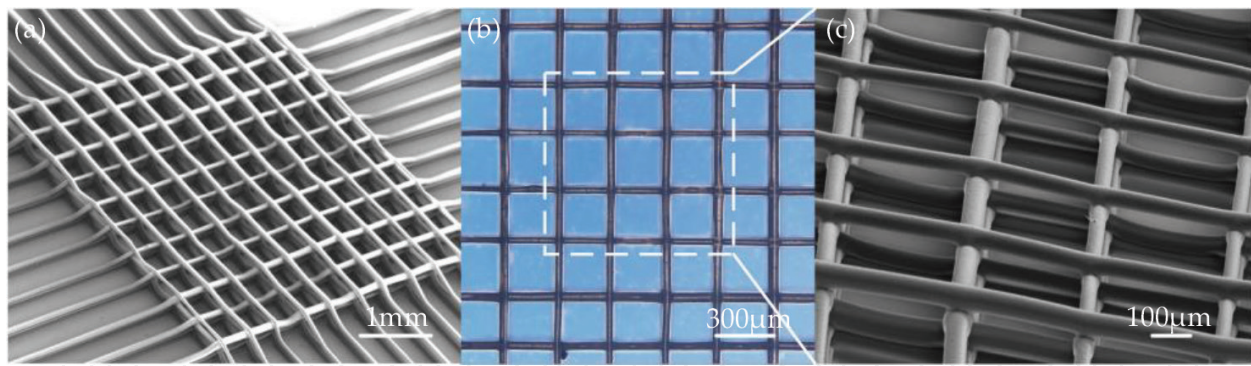


**Figure 13.** A tissue engineering scaffold: (a) overall view; (b) top view; and (c) microview.

#### 4.4. 3D structural electronic (layered heterogeneous structure)

3D structure electronic is a typical multi-material structure product, which is widely used in many fields, such as aerospace, national defense, biological medicine and so on. However, how to realize the manufacturing of 3D structure electronic products with high efficiency and low cost is a very huge challenging problem. The EFD jet deposition 3D printing with multi-nozzle can provide an effective method for the manufacturing 3D electronic. In this case, two kinds of printing materials, photosensitive resin (viscosity 800 mPa s) and conductive silver (viscosity 8000 mPa s), are used. The photosensitive resin is used to construct main body of the 3D structure electronics, while the conductive silver paste is used to print interconnecting wires. The processing parameters of photosensitive resin are printed with voltage 3.2 kV, gas pressure 50 kPa, and moving speed 30 mm/s, while the printing process parameters of conductive silver paste are voltage 2.0 kV, gas pressure 20 kPa, and moving speed 3 mm/s.

As shown in **Figure 14**, the printed structure made of photosensitive resin is a circular platform with a diameter of 7.5 mm at the bottom surface, a diameter of 5.5 mm at the top surface, and a height of 4 mm. There is a printed conductive wire made of conductive silver paste on the top surface of the round platform. Conductive silver paste can be cured at room temperature without heating and other post-processing, which will never damage printed main body of 3D structure electronics.

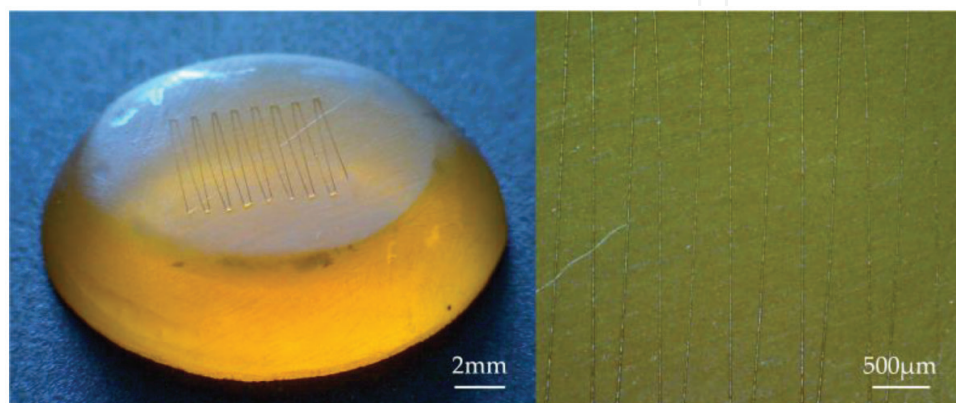


**Figure 14.** A 3D structure electronic device.

Therefore, combining the capability of printing variable materials and the use of multi-nozzle technology, the EFD jet deposition 3D printing presents a very prominent advantage and great potential in the multi-scale and multi-material 3D printing. This technology provides a new solution for the integrated printing of heterogeneous multi-material, multi-scale (macro/micro-scale) structure.

## 5. Conclusion

A novel high-resolution 3D printing, named as high-resolution Electric-field-driven Jet 3D Printing, which is based on the induced electric field and EHD cone-jetting behavior, has been developed to provide a feasible approach to implement additive manufacturing with multi-scale and multi-material. In this chapter, we introduced the system setup and the principle of EFD jet deposition 3D printing. Then, the jetting molding mechanism and influencing rules of operating parameters were revealed by the numerical simulation and verified by the experiments. Finally, four kinds of typical applications including transparent conducting electrodes, high aspect ratio “wall” structure, tissue engineering scaffold, 3D electronics, etc., are presented in detailed. As a result, this new technology offers a novel solution for fulfilling multi-scale and multi-material 3D printing at low cost and good universality as well as high resolution.

## Acknowledgements

This work was financially supported by National Science Foundation of China (Grant No. 51775288) and Key research and development plan of Shandong Province (Grant No. 2018GGX103022).

## Author details

Guangming Zhang, Lei Qian, Jiawei Zhao, Hefei Zhou and Hongbo Lan\*

\*Address all correspondence to: hblan99@126.com

Qingdao Engineering Research Center for 3D Printing, Qingdao University of Technology, Qingdao, Shandong, China

## References

- [1] Wegst U, Bai H, Saiz E, et al. Bioinspired structural materials. *Nature Materials*. 2015; 14:23-36. DOI: 10.1038/nmat4089
- [2] Rosen D, Gibson I, Stucker B. *Additive Manufacturing Technologies*. New York: Springer; 2010. DOI: 10.1007/978-1-4939-2113-3

- [3] Campbell J, McGuinness I, Wirz H, et al. Multimaterial and multiscale three-dimensional bioprinter. *Transactions of the ASME Journal of Nanotechnology in Engineering and Medicine*. 2015;**6**:021005. DOI: 10.1115/1.4031230
- [4] MacDonald E, Wicker R. Multiprocess 3D printing for increasing component functionality. *Science*. 2016;**353**(6307):aaf2093. DOI: 10.1126/science.aaf2093
- [5] Ota H, Emaminejad S, Gao Y, et al. Application of 3D printing for smart objects with embedded electronic sensors and systems. *Advanced Materials Technologies*. 2016;**1**(1):1-8. DOI: 10.1002/admt.201600013
- [6] Truby R, Lewis J. Printing soft matter in three dimensions. *Nature*. 2016;**540**:371-378. DOI: 10.1038/nature21003
- [7] Bartlett N, Tolley M, Overvelde J, et al. A 3D-printed, functionally graded soft robot powered by combustion. *Science*. 2015;**349**(6244):161-165. DOI: 10.1126/science.aab0129
- [8] Wehner M, Truby R, Fitzgerald D, et al. An integrated design and fabrication strategy for entirely soft, autonomous robots. *Nature*. 2016;**536**:451-466. DOI: 10.1038/nature19100
- [9] Lewis J, Ahn B. Device fabrication: Three-dimensional printed electronics. *Nature*. 2015;**518**:42-43. DOI: 10.1038/518042a
- [10] Kong YL, Tamargo IA, Kim H, et al. 3D printed quantum dot light-emitting diodes. *Nano Letters*. 2014;**14**(12):7017-7023. DOI: 10.1021/nl5033292
- [11] Raje PV, Murmu NC. A review on electrohydrodynamic-inkjet printing technology. *International Journal of Emerging Technology and Advanced Engineering*. 2014;**4**:174-183
- [12] Huang Y, Bu N, Duan Y, et al. Electrohydrodynamic direct-writing. *Nanoscale*. 2013;**5**:12007-12017. DOI: 10.1039/C3NR04329K
- [13] Rahman K, Ali K, Muhammad NM, et al. Fine resolution drop-on-demand electrohydrodynamic patterning of conductive silver tracks on glass substrate. *Applied Physics A*. 2013;**111**(2):593-600. DOI: 10.1007/s00339-012-7267-x
- [14] Tse L, Barton K. A field shaping printhead for high-resolution electrohydrodynamic jet printing onto non-conductive and uneven surfaces. *Applied Physics Letters*. 2014;**104**(14):143510-143514. DOI: 10.1063/1.4871103
- [15] Phung TH, Kim S, Kwon KS. A high speed electrohydrodynamic (EHD) jet printing-method for line printing. *Journal of Micromechanics and Microengineering*. 2017;**27**(9):095003(8pp). DOI: 10.1088/1361-6439/aa7c6b
- [16] Mishra S, Barton KL, Alleyne AG, et al. High-speed and drop-on-demand printing with a pulsed electrohydrodynamic jet. *Journal of Micromechanics and Microengineering*. 2010;**20**(20):095026. DOI: 10.1088/0960-1317/20/9/095026



